Chapter 10

Performance Evaluation of HSDPA/HSUPA Systems

Dan Keun Sung and Junsu Kim

Contents

10.1 Introduction 332
10.2 Overall Procedure for Performance Evaluation 332
10.3 Link-Level Simulator 332
10.3.1 Common Function Blocks 332
10.3.2 HSDPA Link-Level Simulation 336
10.3.3 HSUPA Link-Level Simulation 338
10.4 System-Level Simulation 340
10.4.1 System-Level Simulator Structure 340
10.4.1.1 Initialization 341
10.4.1.2 Transmitter (Node B) 345
10.4.1.3 Receiver (UE) 346
10.4.1.4 System-Level Simulator for the HSUPA System 347
10.4.2 Performance Metrics of System-Level Simulations 349
10.4.3 Numerical Examples of System-Level Simulations 350
10.4.3.1 HSDPA System 350
10.4.3.2 HSUPA System 352
10.5 Concluding Remarks 354
References 355

10.1 Introduction

The performance of HSDPA/HSUPA systems is of interest to research engineers to understand the characteristics of the systems and to further enhance performance. Link- and system-level simulations are pratical approaches to evaluate system performance. In this chapter the simulation methodology for the HSDPA/HSUPA systems is described and their performance results are presented.

10.2 Overall Procedure for Performance Evaluation

The overall system performance of HSDPA/HSUPA systems can be evaluated through two simulation steps: one is a *link-level simulation* and the other is a *system-level simulation*. Link-level simulation evaluates the performance of a single air-link between a single transmitter and a single receiver. The performance metrics of link-level simulation include bit error rate (BER), frame error rate (FER), and block error rate (BLER) for varying SINR (signal-to-noise ratio) values. The coding and decoding procedure of the physical layer and mobile radio channels are considered in link-level simulation. The main objective of link-level simulation is to evaluate the performance of a physical-layer coding chain. Therefore, the signal processing functionalities related to radio frequency (RF) blocks, A/D or D/A converting, and sampling functions can be assumed to be ideal.

Unlike link-level simulation, system-level simulation considers multiple transmitters and multiple receivers to analyze the various performance metrics, including throughput, delay, delay variation, etc. It also considers radio resource management schemes, including wireless scheduling, channel allocation, and rate/power control, which are the key functional blocks in determining overall system performance. The link-level simulation results, such as BER, FER, and BLER performance, are utilized in system-level simulation to model each air-link between a transmitter and a receiver. In terms of cell modeling, there is a Node B at the center of the cell and multiple UEs (user equipment) are distributed according to a random distribution. Therefore, a single transmitter (Node B) and multiple receivers (UEs) are implemented for the HSDPA system-level simulator, while multiple transmitters (UEs) and a single receiver (Node B) are considered in the HSUPA system-level simulator.

10.3 Link-Level Simulator

10.3.1 Common Function Blocks

The structure of a link-level simulator is based on a coding chain defined in the technical specifications of the HSDPA and HSUPA systems [1]. Because

the objective of the link-level simulator is to evaluate the link performance of a traffic channel, the coding chains of HS-PDSCH for HSDPA and E-DPDCH for HSUPA are evaluated through link-level simulation. Figure 10.1 shows the overall procedure for HSDPA/HSUPA link-level simulators. Note that the function blocks marked "D" are implemented for HSDPA only. There is a transmitter at the Node B side and a receiver at the UE side in the HSDPA link-level simulator, and vice versa in the HSUPA link-level simulator.

To evaluate the performance of the coding chain, a random binary sequence is generated at the start of simulation. The performance metrics, including BER, FER, and BLER, are measured by comparing the input binary sequence with the decoded binary sequence after decoding. A detailed description for each block is omitted in this chapter. There is a counterpart block at the transmitter for each block at the receiver.

Link-level simulations are performed for various types of mobile radio channels, including AWGN, Rayleigh, ITU defined pedestrian A (PA), pedestrian B (PB), and vehicular A (VA) [2]. In particular the ITU-defined mobile radio channels represent the multi-path fading channels of which tapped-delay-line parameters are shown in Table 10.1. According to the assumption of link-level simulation, each single chip out of spreading sequence can be represented by a single real number because sampling is assumed to be perfect. Therefore, the relative delay of each path is quantized into an integer multiple of chip durations in the link-level simulation. For example, the base chip duration of WCDMA is 260 *ns* because the chip rate is 3.84 Mcps. Then the PA channel in Table 10.1 is modeled as a three-tap multi-path channel because the second and third taps are not resolvable. In other words, the relative delays of the PA channel are converted into an integer multiple of chip durations as follows: tap 1 → zero chip delay; tap 2 → one chip delay; tap 3 → one chip delay, tap 4 → 2 chips delay.

Figure 10.2 provides an example of link-level multi-path processing for the ITU-PA channel. Although four paths are defined in the PA channel, taps 1 and 2 have the same delay in terms of chip duration, as shown in the figure. The spread sequence for symbol k is delayed and distorted through the multi-path channel. Finally, the receiver obtains an aggregated sequence containing all the components of the different propagation paths. Multiple fingers at the RAKE receiver perform correlations to gather the signal energy of symbol k.

Figure 10.3 illustrates a RAKE receiver structure. The receiver can receive multiple distorted and delayed replicas of the transmitted radio frame due to the multi-path fading channel that causes inter-symbol interference (ISI). The *multi-path searcher and tracker* resolves each replica of the transmitted signal at the first step of the receiver, as shown in Figure 10.3. Using fingers, it is possible to resolve more paths. The distorted phase of each path is compensated by the *phase compensator* using the phase distortion

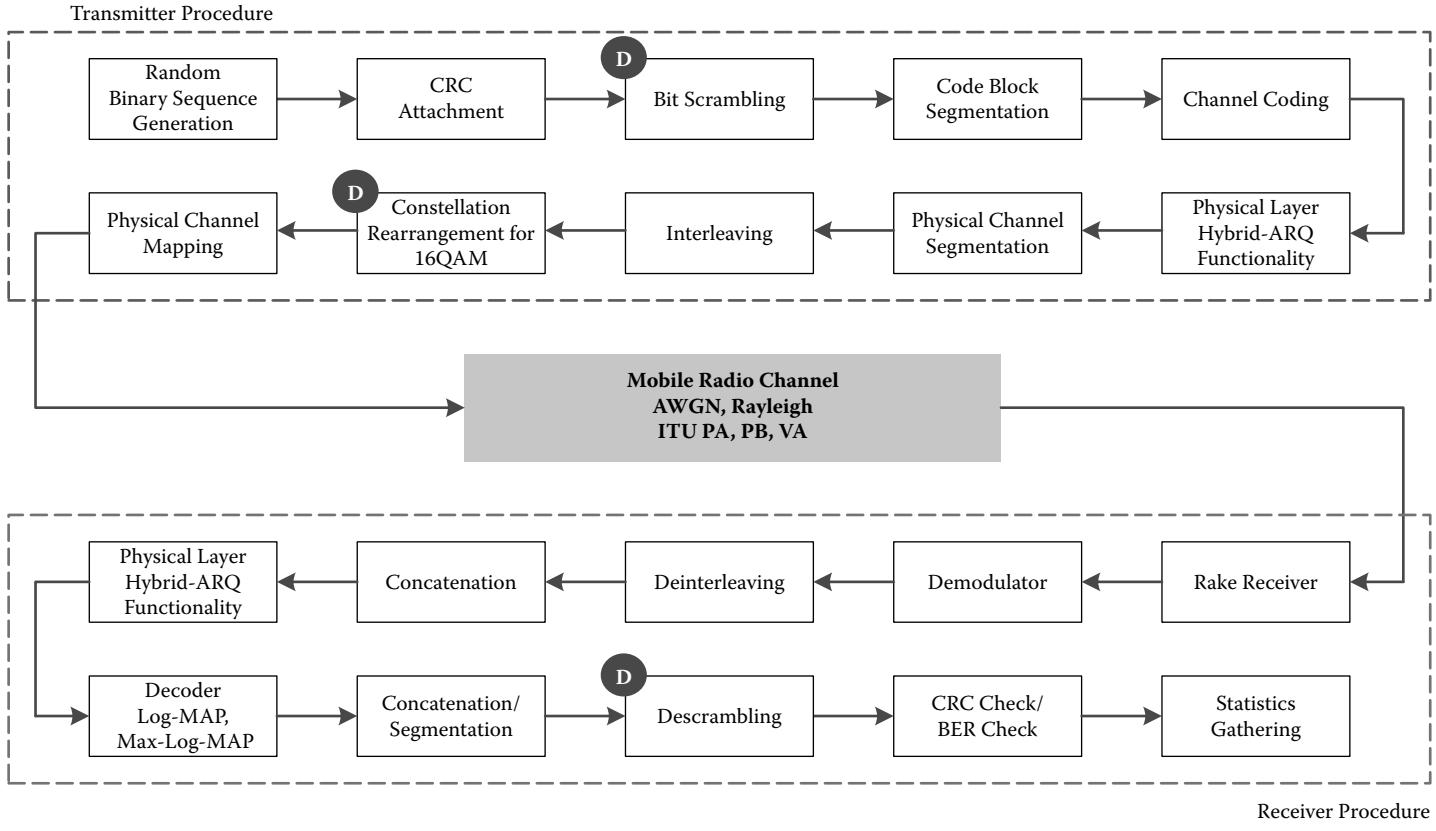

Figure 10.1 Procedure for HSDPA/HSUPA link-level simulation. D denotes HSDPA only.

Table 10.1 Parameters for ITU Mobile Radio Channels

	PA		PB		VA	
Tap	Relative Delay (ns)	Average Power (dB)	Relative Delay (ns)	Average Power (dB)	Relative Delay (ns)	Average Power (dB)
1	0	0.0	0	0.0	0	0.0
2	110	−9.7	200	−0.9	310	−1.0
3	190	−19.2	800	−4.9	710	−9.0
4	410	−22.8	1200	−8.0	1090	−10.0
5	—	—	2300	−7.8	1730	−15.0
6	—	—	3700	−23.9	2510	−20.0

information estimated by a *channel estimator*. Because the main objective of this link-level simulation is to evaluate the performance of the coding chain shown in Figure 10.1, we can assume a perfect channel estimation at the RAKE receiver. Finally, multiple *correlators* produce de-spread signals, and they are combined by a *multi-path combiner*. The combined signal is provided to the remainder of a decoding chain to obtain the decoded binary sequence.

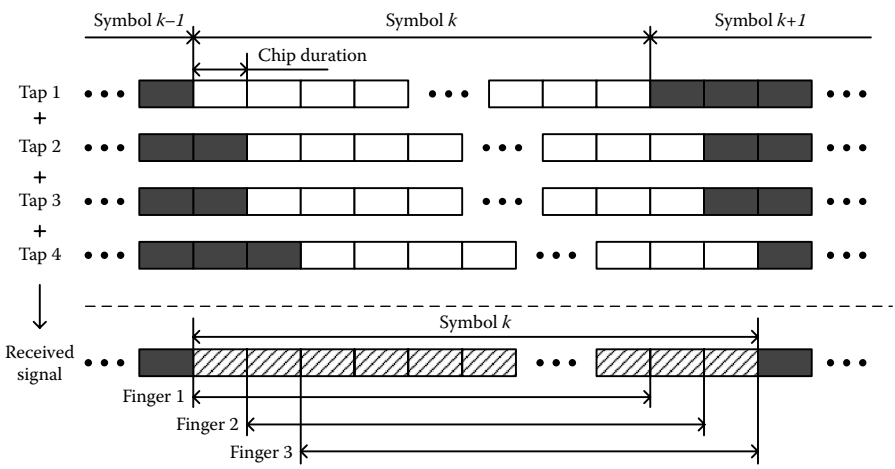

Figure 10.2 Example of multi-path processing with ITU-PA.

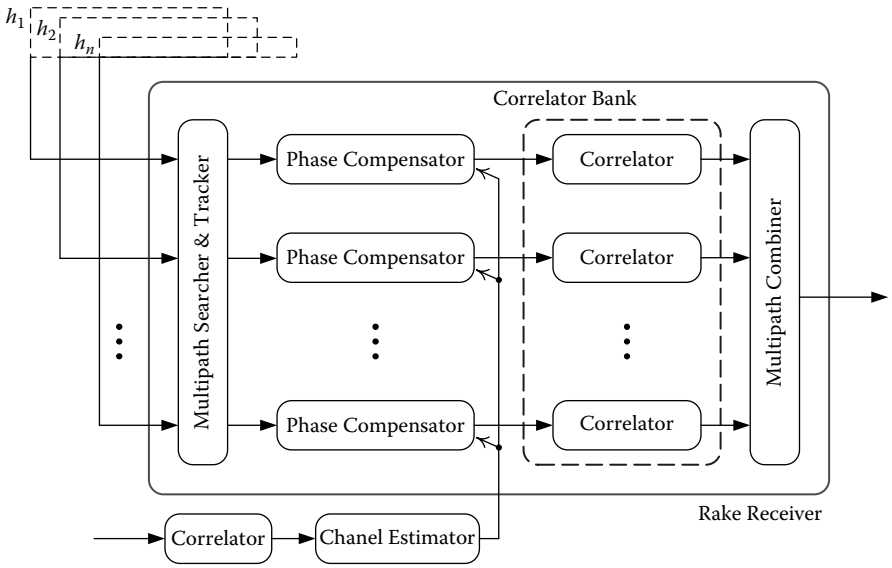

Figure 10.3 RAKE receiver structure.

10.3.2 HSDPA Link-Level Simulation

The HSDPA system supports QPSK and 16-QAM modulations, convolutional and turbo codes for channel coding, and multi-code transmission. There are various combinations of modulation and coding schemes and a number of multi-codes. Each combination is characterized as a channel quality indicator (CQI) [3]. The *CQI value* represents the *adaptive modulation and coding* (AMC) *level* generally used in wireless communications. Because a higher CQI value indicates a higher modulation order and weaker channel coding, it is possible to achieve a successful transmission with the higher CQI value only when the wireless channel status is sufficiently good. Therefore, the CQI value can be used as a good indicator representing the channel quality of each UE.

The HSDPA system defines a different CQI mapping table for a different category of UEs. The category is determined according to the capability of UE [4]. Categories 1 to 6 support up to 16-QAM and five multi-code transmission, Categories 7 and 8 support up to 16-QAM and ten multi-code transmission, Category 9 supports up to 16-QAM and 12 multi-code transmission, Category 10 supports up to 16-QAM and 15 multi-code transmission, and Categories 11 and 12 support QPSK only and up to five muti-code transmission. Among the twelve categories, Category 10 presents a maximum data rate of approximately 12.8 Mbps. Table 10.2 shows the representative CQI values for UE Category 10 [3]. The CQI values from 1 to 30 are defined

Table 10.2 Representative CQI Values for UE Category 10

CQI Value	*Transport Block Size*	*Number of HS-PDSCH*	*Modulation Type*
0	N/A	Out of range	
1	237	1	QPSK
. . .	. . .	. . .	. . .
7	650	2	QPSK
. . .	. . .	. . .	. . .
10	1262	3	QPSK
. . .	. . .	. . .	. . .
13	2279	4	QPSK
. . .	. . .	. . .	. . .
15	3319	5	QPSK
16	3565	5	16-QAM
. . .	. . .	. . .	. . .
23	9719	7	16-QAM
24	11418	8	16-QAM
25	14411	10	16-QAM
26	17237	12	16-QAM
27	21754	15	16-QAM
. . .	. . .	. . .	. . .
30	25558	15	16-QAM

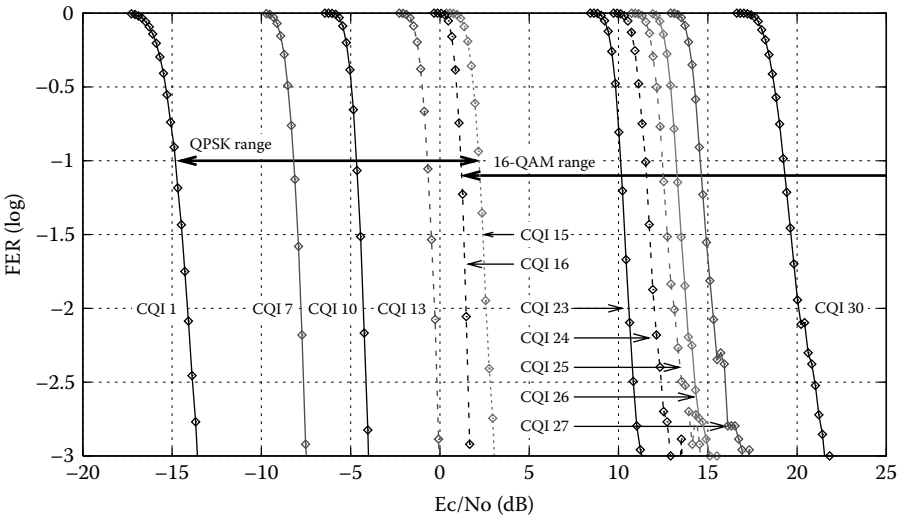

Figure 10.4 FER performance of the HSDPA system under a Rayleigh fading channel.

for data transmission, and CQI 0 indicates out-of-range status. For each CQI value, various parameters for the coding chain depicted in Figure 10.1 are determined. Therefore, it is possible to analyze the link performance for 30 CQI values.

Figure 10.4 depicts the FER performance of the HSDPA system for various CQI values under a Rayleigh fading channel. Higher values of CQI require more energy to achieve a certain level of FER. However, CQI 15 requires more energy than CQI 16 in a Rayleigh fading channel. CQI 15 is the maximum CQI for QPSK modulation, and CQI 16 is the minimum CQI for 16-QAM modulation. Therefore, CQIs 15 and 16 are in the overlapping area of the dynamic ranges of the QPSK and 16-QAM. If the required FER is set to 10%, a transition from QPSK to 16-QAM occurs at approximately 3 dB of Ec/No. This result is used in the system-level simulations for CQI selection and ACK/NACK decision.

10.3.3 HSUPA Link-Level Simulation

One radio frame for E-DPDCH contains five sub-frames, and each sub-frame has three slots. Therefore, one radio frame consists of 15 slots. The HSUPA system defines eight different slot formats that control the transmission rate by adjusting the spread factor (SF) from 2 to 256. Table 10.3 shows the slot formats [5]. Using the slot format shown in Table 10.3, several transmission format combinations (TFCs) are possible. In particular, E-DCH Category 6

Table 10.3 E-DPDCH Slot Formats

Slot Format	*Channel Bit Rate (kbps)*	*SF*
0	15	256
1	30	128
2	60	64
3	120	32
4	240	16
5	480	8
6	960	4
7	1920	2

allows up to four multi-code transmission for both 2-ms and 10-ms TTI [4]. Table 10.4 shows the TFC for Category 6. TFCs 0 to 6 use a single code transmission. TFC 7 transmits two SF4 channels, TFC 8 transmits two SF2 channels, and TFC 9 transmits two SF2 channels and two SF4 channels. In link-level simulation, the link performance can be analyzed for each

Table 10.4 Transmission Format Combinations (TFCs) for Category 6

Index	*Bit Rate (kbps)*	*Combination*	*Bits/Frame*	*Bits/Sub-frame*	*Bits/Slot*
0	15	SF256	150	30	10
1	30	SF128	300	60	20
2	60	SF64	600	120	40
3	120	SF32	1200	240	80
4	240	SF16	2400	480	160
5	480	SF8	4800	960	320
6	960	SF4	9600	1920	640
7	1920	2×SF4	19200	3840	1280
8	3840	2×SF2	38400	7680	2560
9	5760	2×SF2 + 2×SF4	57600	11520	3840

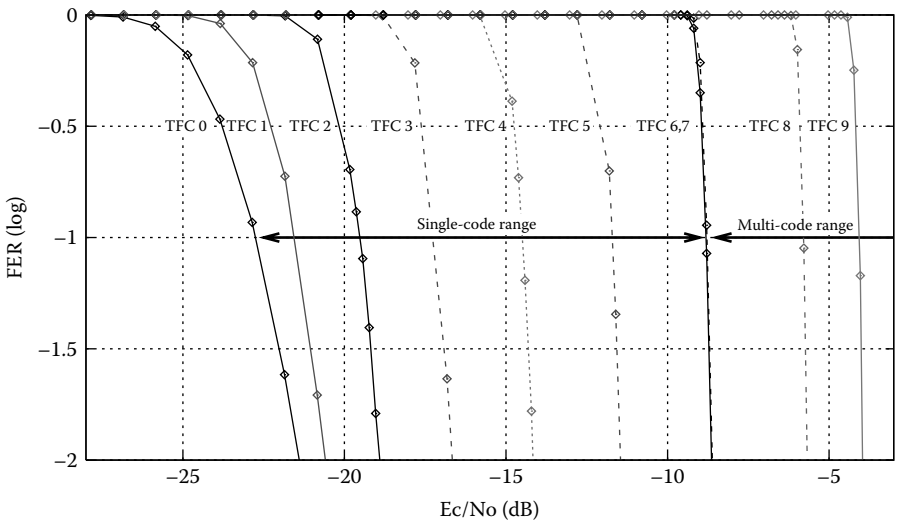

Figure 10.5 FER performance of the HSUPA system under a Rayleigh fading channel.

TFC in Table 10.4 using the parameters for frame (10 ms) or sub-frame (2 ms).

Figure 10.5 depicts the FER performance of the HSUPA system under a Rayleigh fading channel with 10-ms TTI. TFC 6 has a single code transmission with spreading factor 4 and TFC 7 has a two-code transmission with spreading factor 2. Both TFCs have nearly identical FER performance under a Rayleigh fading channel. However, TFC 7 transmits twice more data than TFC 6. Therefore, TFC 7 is selected rather than TFC 6 in system-level operation.

10.4 System-Level Simulation

10.4.1 System-Level Simulator Structure

The entire structure and major function blocks for the HSDPA system-level simulator is described here. Figure 10.6 represents the structure of a system-level simulator for the HSDPA system. Unlike the link-level simulator, the system-level simulator focuses on the system-level performance among multiple transmitters and multiple receivers in a multi-cell environment. The functional blocks of the system-level simulator can be grouped into three parts: initialization, transmitters (Node B), and receivers (UE).

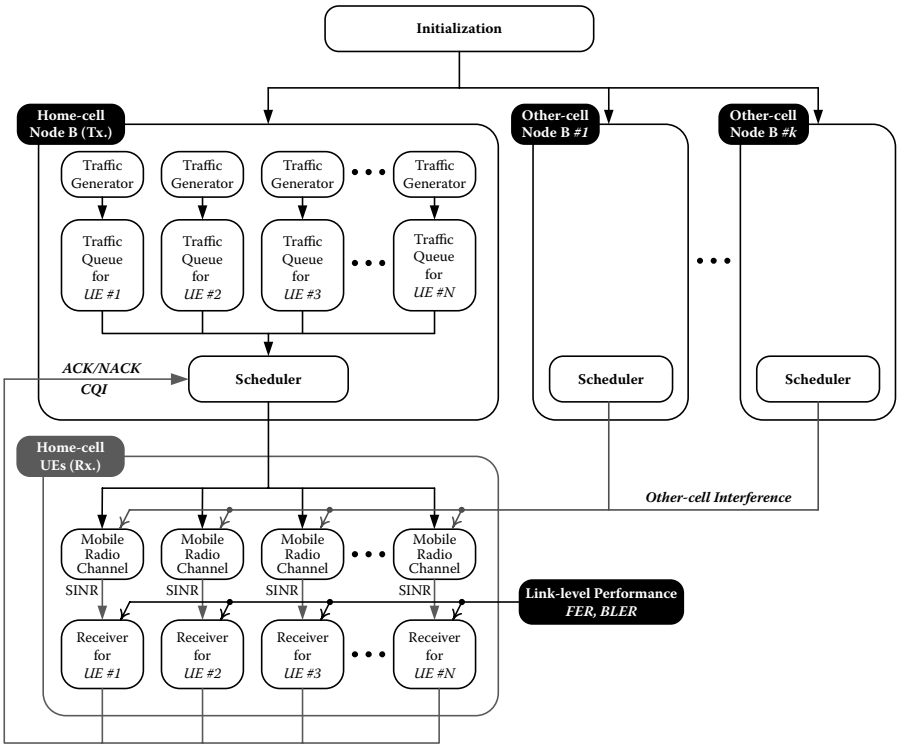

Figure 10.6 System-level simulator structure for the HSDPA system.

10.4.1.1 Initialization

10.4.1.1.1 Topology

The geographical positions of Node Bs and UEs are fixed throughout the simulation. Node Bs have deterministic locations while the positions of UEs are randomly distributed. Generally, a hexagonal cell structure is considered, and one Node B in a single-cell environment, seven Node Bs in a single-tier environment, and 19 Node Bs in a two-tier environment are implemented. Figure 10.7 shows a multi-cell model representing a home-cell, the first-tier, and the second-tier cellular environments [6]. A home-cell Node B is located at the center.

Positioning UEs follow either a uniform distribution or a Gaussian distributions. A Gaussian distribution model effectively represents an environment in which more UEs are concentrated in a cell center area. On the other hand, if UEs are located according to the uniform distribution, then more users are located in a cell boundary area. Generally, the uniform distribution model yields much poorer system-level performance than the Gaussian distribution model.

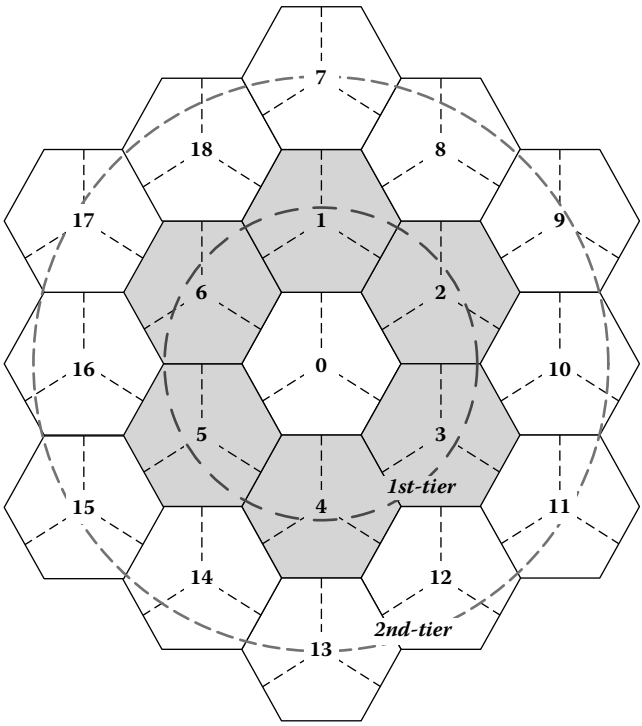

Figure 10.7 Multi-cell model.

10.4.1.1.2 Static Channel (Large-Scale Fading) Parameters

Once the locations of Node Bs and UEs are set, then static channel parameters are also determined. The static channel parameters, which represent the mobile radio channel components depending only on the geographical environment, include path loss, shadowing, antenna gain, etc.

A path-loss (PL) model widely used in urban and suburban areas can be expressed as [2,7]

$$PL[\text{dB}] = 40(1 - 4 \times 10^{-3} h_{BS}) \log_{10}(R) - 18 \log_{10}(h_{BS}) + 21 \log_{10}(f) + 80 \tag{10.1}$$

where R is the distance in kilometers from Node B to a UE, f is the carrier frequency in megahertz, and h_{BS} is the height of Node B above rooftop. For HSDPA/HSUPA with 2-GHz carrier frequency, if h_{BS} is set to 15 m above rooftop, then the path-loss formula becomes

$$PL(R)[\text{dB}] = 128.1 + 37.6 \log_{10}(R) \tag{10.2}$$

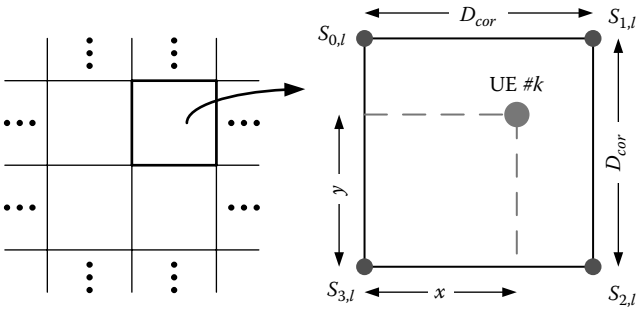

Figure 10.8 Shadowing factor grid.

The shadowing factor (SF) can be modeled using a log-normal distribution, and its standard deviation depends on the given propagation scenario. In urban or suburban macrocells, the standard deviation is set to 8 dB [7]. Because the shadow fading is caused by geographical environment, including buildings, hills, trees, and so on, the shadowing factors of the adjacent UEs are correlated. The longest distance between the UEs within which the correlation is maintained is called the *decorrelation distance*. Therefore, the shadowing factor of each UE should be generated according to the predefined decorrelation distance [7]. Figure 10.8 shows a shadowing factor grid to generate the correlated shadowing factor. The entire plane, including the home-cell shown in Figure 10.7, can be divided into multiple squares. The length and height of a single square are equal to the decorrelation distance D_{cor}, as shown in the right figure, and UE *#k* is located in the square. $S_{0,l}, \cdots, S_{3,l}$ at the four nodes of the square are the Gaussian distributed random variables with a standard deviation mentioned above. The $S_{n,l}$, which denotes the shadowing factor at node n and Node B l, is generated as $aZ_n + bZ_l$, where Z_n is a Gaussian random number for each node, Z_l is a Gaussian random number for each Node B, and $a^2 = b^2 = 1/2$. Then, the shadowing factor of UE *#k* can be calculated using the following interpolation [7]:

$$SF[\text{dB}] = \sqrt{1 - \frac{x}{D_{cor}}}\left(S_{0,l}\sqrt{\frac{y}{D_{cor}}} + S_{3,l}\sqrt{1 - \frac{y}{D_{cor}}}\right) + \sqrt{\frac{x}{D_{cor}}}\left(S_{1,l}\sqrt{\frac{y}{D_{cor}}} + S_{2,l}\sqrt{1 - \frac{y}{D_{cor}}}\right) \tag{10.3}$$

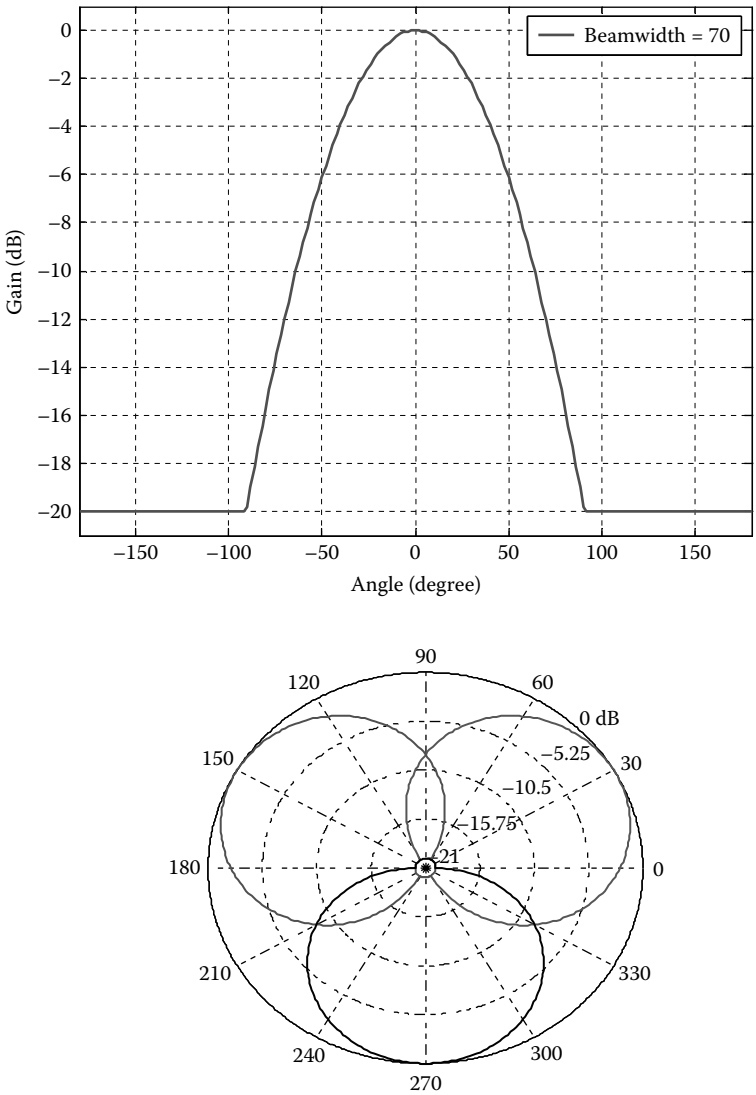

Figure 10.9 Antenna pattern for sectorization.

Figure 10.9 illustrates an antenna pattern for sectorization. The antenna gain $AG(\theta)$, shown in the upper figure of Figure 10.9, is generated as

$$AG(\theta)[\text{dBi}] = -\min\left\{12\left(\frac{\theta}{\theta_{3dB}}\right)^2, A_m\right\} \tag{10.4}$$

where θ is the relative direction to the main robe, $-180° \leq \theta \leq 180°$, θ_{3dB} is the 3-dB beamwidth, and $A_m = 20$ dB is the maximum attenuation. The typical value of θ_{3dB} is 70° for a three-sector antenna system [6]. The lower figure of Figure 10.9 shows a sectorization using the antenna pattern of Equation (10.4) in a cell. The directions of main lobes are 30°, 150°, and 270°.

Finally, the large-scale fading gain G_{LS} at a UE is expressed as

$$G_{LS}[dB] = -PL - SF + AG \tag{10.5}$$

Note that the path loss and shadowing factor in Equations. (10.1) and (10.3) have positive values, and the antenna gain in Equation (10.4) has a negative value. Therefore, the large-scale fading gain G_{LS} has a negative value. G_{LS} is maintained unless the UE's position is changed.

10.4.1.2 Transmitter (Node B)

10.4.1.2.1 Traffic Generator and Traffic Queue

At Node B, there is a traffic generator and a traffic queue for each UE. The traffic types generally used for system-level simulations include full-queue, HTTP, FTP, VoIP, near-real-time video (NRTV), gaming, e-mail, and so on [6,7]. Unlike the other traffic types, full-queue traffic represents that a sufficient amount of traffic is always backlogged in the traffic queue. If full-queue traffic is applied, because there are no effects of queuing dynamics on the system performance, it is desirable to evaluate the maximum performance bound of the system.

The traffic generator produces packets containing the information about generation time and packet length which are used for measuring packet delay and throughput, respectively. The generated packets are stored in a FIFO-type traffic queue awaiting for scheduling.

10.4.1.2.2 Scheduler

The scheduler is one of the most important functions that affect system performance. The function of the scheduler is to select a UE to serve at every TTI. For the operation, the scheduler utilizes ACK/NACK and CQI feedback information from UEs and the backlogging status of each UE's traffic queue.

Because the HSDPA system adopts HARQ, a UE with NACK feedback has the highest priority for scheduling. Therefore, the scheduler always serves the UE with NACK feedback until ACK occurs or the retransmission counter expires. Generally, the number of retransmissions is limited to three or four. Once the retransmission counter value exceeds the retransmission limit, the packet is discarded and the counter is reset.

If there are no UEs with NACK feedback, then the scheduler orders and selects the UEs according to its own scheduling criterion. Well-known scheduling algorithms include Max C/I (or best SINR) and Proportionally Fair (PF) algorithms. The Max C/I scheduler selects one UE with the best SINR value. In the HSDPA system, UEs report CQI values instead of the measured SINR values. The reported CQI values can be considered as a quantized version of the SINR values. Therefore, the Max C/I scheduler simply chooses one UE with the highest CQI value among all UEs in a cell. Because the Max C/I selects the UE with the best channel quality, it can be used for evaluating the maximum limit of system throughput. However, due to a fairness problem, the Max C/I scheduler is not a feasible solution for the practical HSDPA system. The PF scheduler can be a feasible solution for solving the fairness problem while minimizing throughput degradation. The PF scheduler can be implemented using the normalized SINR algorithm, which selects one UE with the largest value of the instantaneous SINR normalized by the long-term average of its own SINR. Therefore, the PF for the HSDPA system can be implemented using the normalized CQI instead of the normalized SINR.

10.4.1.3 Receiver (UE)

10.4.1.3.1 SINR Measurement

Every UE measures the SINR value at each TTI. The desired signal is transmitted from the home-cell Node B and the interference comes from the other cells. The received SINR value of UE k, $z(k)$, can be measured as

$$z(k) = \frac{G_{LS}^{hc} G_{SS}^{hc} P_{tx}^{hc}}{N_0 W + LF \cdot \sum_{\text{other-cells}} G_{LS}^{oc} G_{SS}^{oc} P_{tx}^{oc}}, \tag{10.6}$$

where the superscripts hc and oc represent the home-cell and other-cell, respectively, G_{LS} is the large-scale fading gain, G_{SS} is the small-scale fading gain, P_{tx} is the transmit power, N_0 is the noise spectral density, W is the channel bandwidth, and LF is the loading factor of the other-cells. For more accurate simulations, other-cells need to be modeled reflecting the transmissions and reception of UEs with the corresponding Node Bs. However, it is too complex to simulate these operations. Therefore, it is assumed that UEs are located in the home-cell only, and the transmit power of the other-cell NodeB, P_{tx}^{oc} is constant. To evaluate the effect of other-cell interference level, the loading factor (LF) is used for adjusting the level. The LF is a real number in [0, 1].

Once the position of the UE is determined, the large-scale fading gains, G_{LS}^{hc} and G_{LS}^{oc}, are also determined according to Equation (10.5). The noise

power term is also constant. Therefore, only the small-scale fading gains, G_{SS}^{bc} and G_{SS}^{oc}, are generated at every measurement time. The small-scale fading gain depends on the given type of mobile radio channel. G_{SS} is 1 for the AWGN channel. For the independent Rayleigh fading channel, $\sqrt{G_{SS}}$ is a Rayleigh-distributed random variable. If the time-correlated Rayleigh fading channel is required, then $\sqrt{G_{SS}}$ is generated using Jakes' model. Other fading models, including Rician channel and Nakagami-m channel, also can be used.

10.4.1.3.2 CQI Determination

Each UE determines the proper CQI value based on the measured SINR value and reports it to the home-cell Node B at every TTI. The UE should select the highest CQI value with which the frame can be successfully received while satisfying a required FER of 0.1 [3]. For example, if the current measured SINR is 0 dB in Figure 10.4, then the UE selects CQI 13 because it is the highest CQI value among the CQI values achieving the required FER of 0.1.

10.4.1.3.3 HARQ Process and ACK/NACK Decision

The UE that received a frame decides ACK or NACK using the measured SINR. The estimated FER value is obtained from the link-level simulation result using the current SINR. Then, the system-level simulator generates a random number in (0, 1) using the uniform distribution and decides NACK if the random number is smaller than the given FER. ACK is decided in the other case. The ACK/NACK information is reported to Node B. If Node B receives NACK, then it retransmits the previous frame. There are two types of HARQ processes: chase-combining (CC) and incremental redundancy (IR). For the CC-type HARQ, Node B retransmits the same information and parity bits. Therefore, the CQI value of the retransmitted data is the same as the original (previous) transmission, and SINR gain can be obtained through retransmissions at the receiver. On the other hand, the IR-type HARQ uses different coding for each retransmission. Therefore, the distinct FER curve for each retransmission format is required to evaluate the system performance of the IR-type HARQ.

10.4.1.4 System-Level Simulator for the HSUPA System

Unlike the HSDPA system, multiple UEs act as transmitters in uplink and a home-cell Node B acts as a receiver as shown in Figure 10.10. Therefore, a traffic generator and traffic queue are located in each UE. The UEs transmit their data according to the absolute or relative grant information from an uplink scheduler in Node B. The uplink scheduler adjusts each UE's

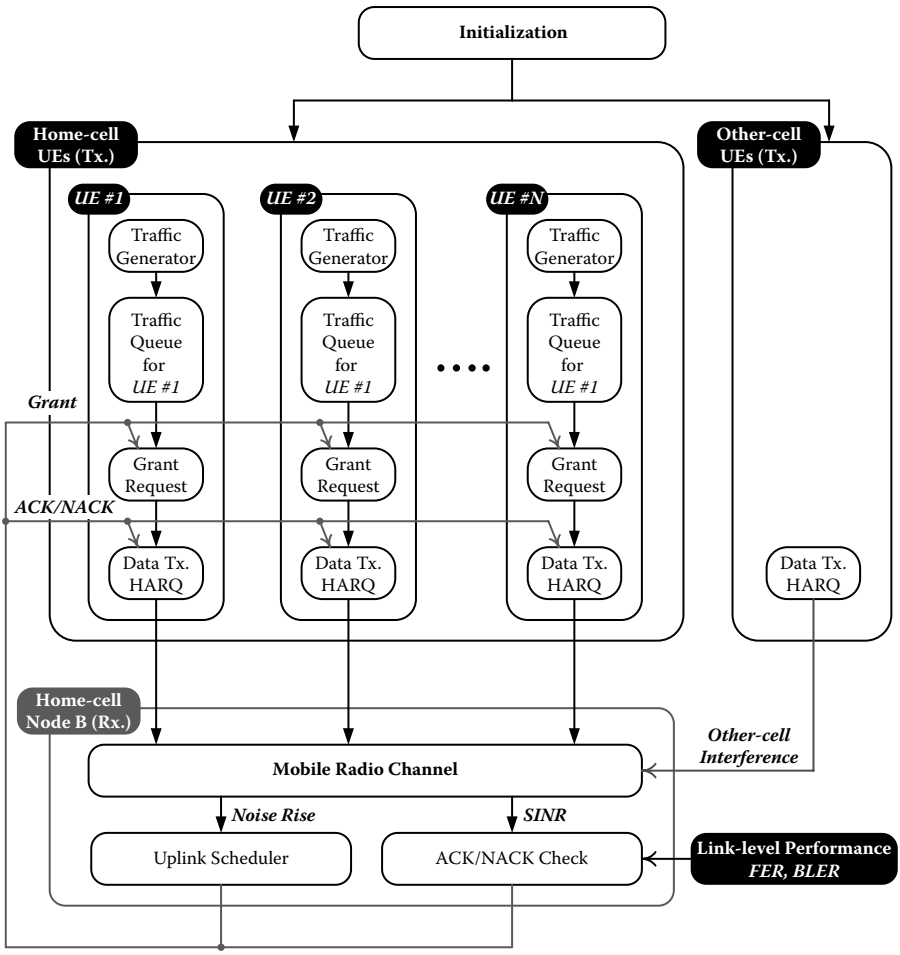

Figure 10.10 System-level simulator structure for the HSUPA system.

transmission format using the grant message for maintaining the overall noise rise in the home-cell below the allowable noise rise. Node B is also responsible for determining ACK/NACK for HARQ.

In the HSUPA system-level simulator, a number of UEs in other-cells act as interferers. To reduce computational complexity, it is required to approximate a single interference source instead of simulating a number of individual interferers in other-cells. According to the central limit theorem, the sum of a number of interferences can be approximated by the Gaussian distribution. The mean and variance of the Gaussian distribution can be varied according to the other-cell interference status.

10.4.2 Performance Metrics of System-Level Simulations

Throughput and delay are the most important performance metrics for system-level simulation. According to the different measurement perspectives, various metrics can be defined as follows:

- *System throughput* represents the total amount of successfully transmitted data during the simulation time. Let b_u denote the successfully transmitted data of user u in bits; then the system throughput R_{sys} can be expressed as

$$R_{sys} = \frac{\sum_{\forall u}^{N_{user}} b_u}{\tau_{sim}} \tag{10.7}$$

  where N_{user} represents the total number of users and τ_{sim} is the total simulation time, respectively.
- *Spectral efficiency* is scaled version of the system throughput expressed as

$$R_{eff} = \frac{R_{sys}}{BW} \tag{10.8}$$

  where BW is the system bandwidth in hertz.
- *Average user throughput* is defined as

$$R_{user} = \frac{R_{sys}}{N_{user}} \tag{10.9}$$

- *Average packet call throughput* is measured for some specific traffic models having packet call, such as VoIP traffic model [6,7]. Packet call throughput is the total bits per packet call divided by total packet duration. Then the average packet call throughput can be expressed as

$$R_{call} = \sum_{\forall u}^{N_{user}} \frac{1}{N_{call,u}} \sum_{\forall i}^{N_{call,u}} \frac{b_{u,i}}{\delta_{u,i}} \tag{10.10}$$

  where $N_{call,u}$ denotes the number of packet calls for user u, $b_{u,i}$ represents the successfully transmitted bits in the ith packet call for user u, and $\delta_{u,i}$ is the duration of ith packet call for user u.
- *Average user packet call throughput* is defined as

$$R_{call,user} = \frac{R_{call}}{N_{user}} \tag{10.11}$$

- *Average packet delay* is the average time duration for successful transmission of each packet. According to the length of a packet, it can be fragmented into several segments for transmission. Then, the packet delay is measured from the start of the first segment until the every segment is delivered to the receiver. If some of the segments are discarded during the HARQ process, then the entire packet transmission is failed and the packet is also discarded. Therefore, the packet delay only considers the successfully transmitted packets.

In addition to the itemized performance metrics above, there can be various performance metrics, including the received SINR distribution, distribution for the number of retransmission, CQI/TFC distribution, service probability, delay variation, and so on.

10.4.3 Numerical Examples of System-Level Simulations

10.4.3.1 HSDPA System

Figure 10.11 shows the system throughput for HSDPA when the full-queue traffic model, Max C/I scheduler, and Rayleigh fading channel are used for system-level simulations. The UE Category 10 shown in Table 10.2 is assumed, and link-level simulation results in Figure 10.4 are used for CQI determination and ACK/NACK decision. Because a home-cell has three sectors, the total cell throughput is three times the average sector throughput. The full-queue traffic model implies that every UE's traffic queue is always backlogged with a sufficient amount of traffic. This traffic model is generally used in a bid to analyze the maximum throughput performance of the system because the queuing dynamics according to the activity of the traffic pattern are not considered.

Figure 10.11 also shows the system throughput for different MIMO configurations that the HSDPA supports. The "No Diversity" in the figure represents the normal antenna configuration, which is one transmit antenna in the Node B and one receive antenna at the UE. HSDPA supports two types of transmit diversity schemes: space-time transmit diversity (STTD) and closed-loop transmit diversity (CLTD). Because CLTD uses the feedback information from the UE, more SNR gain can be achieved, as shown in the figure.

High system throughput performance is achieved through the wireless scheduler, which provides a multi-user diversity (MUD) gain. Figure 10.12 shows examples of the MUD gain achieved by the Max C/I scheduler. This figure presents the received SINR distributions for all users and for the selected users by the scheduler. Because the Max C/I scheduler selects the users with the best channel quality at each time, the SINR values of the

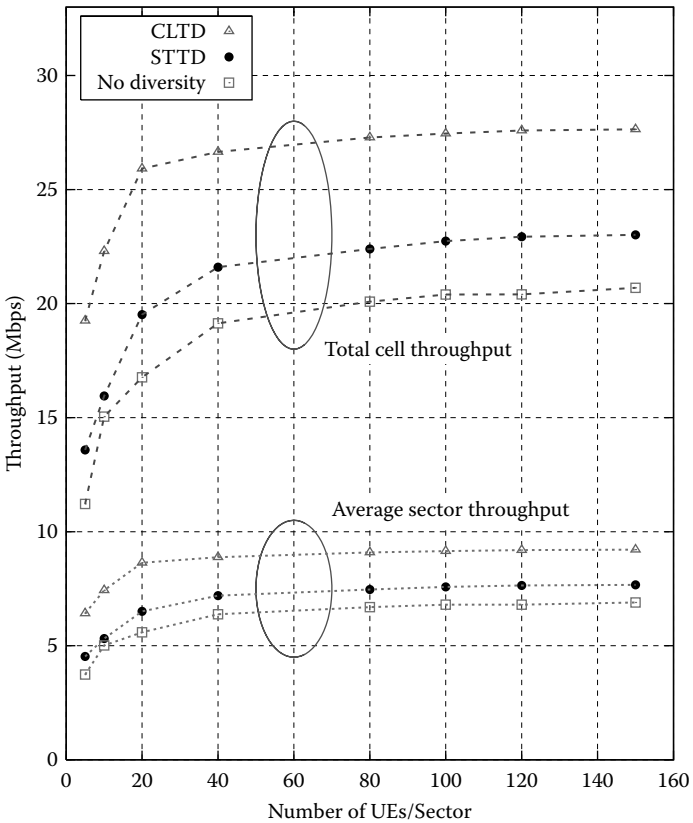

Figure 10.11 System throughput for the HSDPA, Rayleigh fading channel.

scheduled users become higher, as shown in the figure. Moreover, as the number of users increases, the MUD gain also increases.

The Max C/I provides the maximum MUD gain to maximize the system throughput while it does not consider the fairness among the users. It is possible to observe the fairness of each scheduling algorithm in Figure 10.13. This figure shows the service probability according to the distance from the Node B. The service probability is defined as the probability that a UE at a certain location is scheduled. Because the selection criterion of the Max C/I scheduler is based on the SINR value, as the UE is located far from the Node B, the service probability also decreases drastically. However, the PF scheduler is based on the normalized SINR instead of the SINR itself. Therefore, the service probability is nearly even regardless of the distances, as shown in the figure. While the PF scheduler provides a fair service, the MUD gain is degraded.

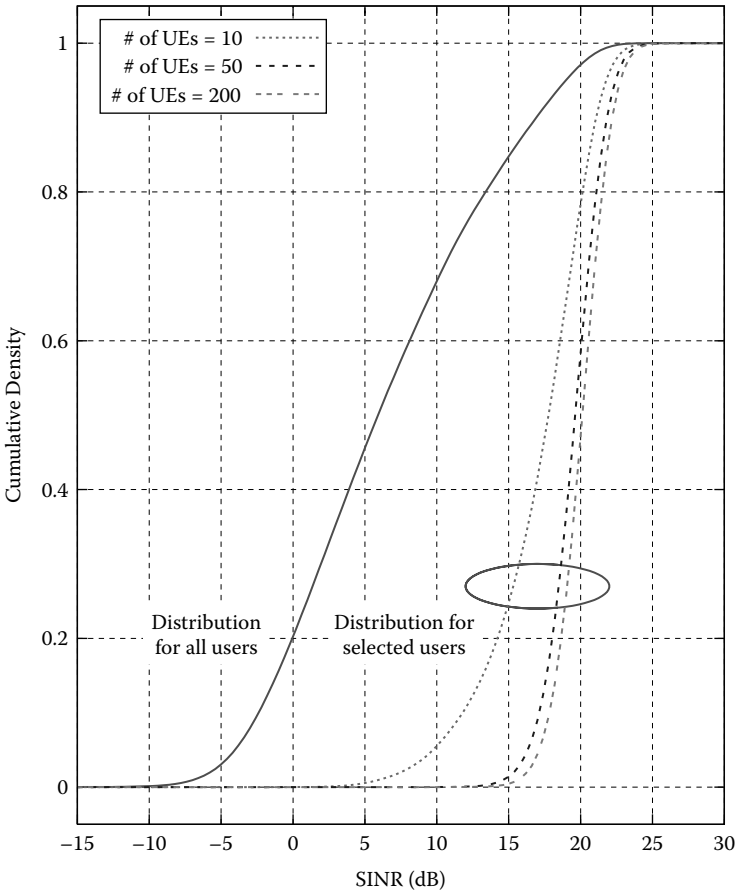

Figure 10.12 SINR distributions before and after scheduling, Rayleigh fading channel.

10.4.3.2 HSUPA System

The TFC formats shown in Table 10.4 are used to evaluate the performance of the HSUPA system. Figure 10.14 shows the system throughput performance of HSUPA with full-queue traffic in Rayleigh fading channel. The code-domain uplink scheduling is performed with the maximum allowable noise rise of 5 dB. As the number of UEs increases, the system throughput decreases. This is a different characteristic from the HSDPA system. Because the HSUPA is an uplink system, the aggregated interference at Node B (receiver) as the number of UEs (transmitters) increases. The total amount of the interference, which is measured as the *noise rise*, is controlled to be less than the target value, which is 5 dB in this case. The scheduler orders

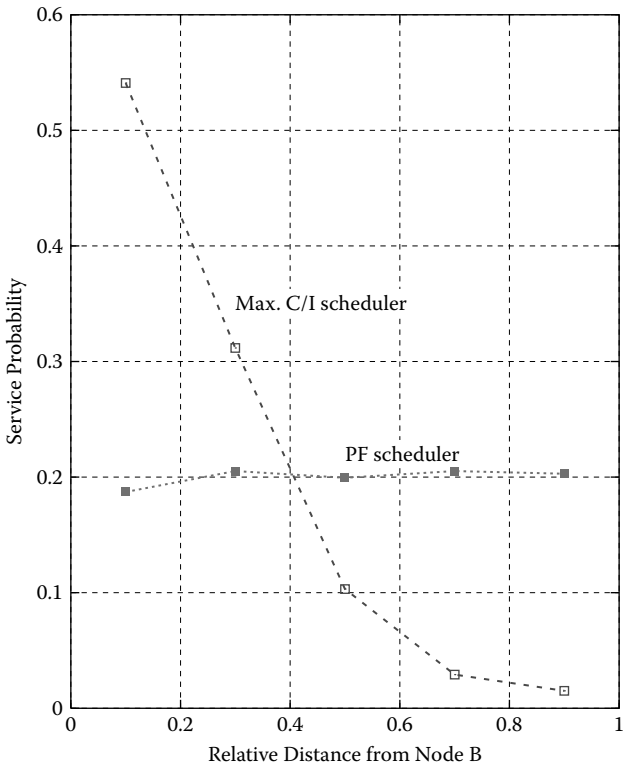

Figure 10.13 Service probabilities for two different schedulers, Rayleigh fading channel.

the UEs to lower their TFC through the absolute/relative grant process in order to support as many UEs as possible while maintaining the noise rise requirement. Consequently, the system throughput decreases as the number of UEs increases because the transmit power of each UE decreases and the total interference at Node B increases.

Figure 10.15 illustrates the system throughput of the HSUPA system when the VoIP traffic model is used. Comparing to Figure 10.14, the system throughput increases as the number of UEs increases. The VoIP traffic is generated periodically with an on/off pattern and a rate of approximately 10 kbps. Due to the relatively low rate and activity of the VoIP traffic, it is possible to maintain a low level of interference. Therefore, the system throughput increases as the number of UEs increases. Because the uplink is sensitive to the interference among the UEs, the HSUPA system is appropriate to serve medium/low rate data services, including VoIP and streaming video traffic.

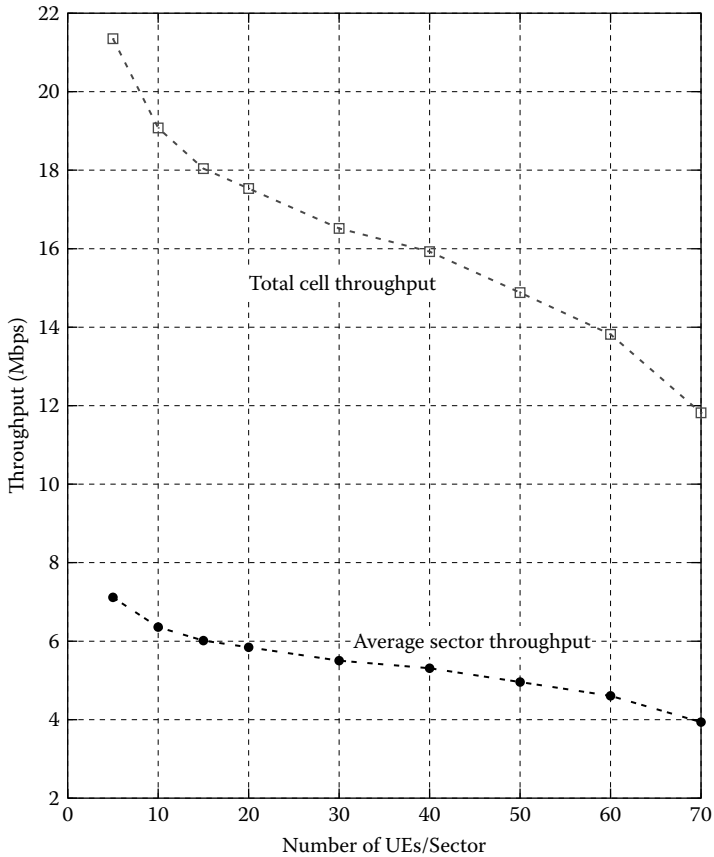

Figure 10.14 System throughput for the HSUPA, full queue traffic.

10.5 Concluding Remarks

The performance of the HSDPA/HSUPA system is evaluated through link- and the system-level simulators. The link-level simulation provides the performance of a single link between a transmitter and a receiver. The system-level simulator evaluates the performance of the system with multiple transmitters and multiple receivers in a multi-cell environment by considering the radio resource management (RRM) schemes, such as scheduling, rate control, and power control.

The HSDPA/HSUPA system achieves MUD gain through an opportunistic scheduler and yields high throughput. Through the simulator, it is possible to analyze the achievable MUD gain for the Max C/I and PF scheduling algorithms. Moreover, the fairness of each scheduler also can be evaluated.

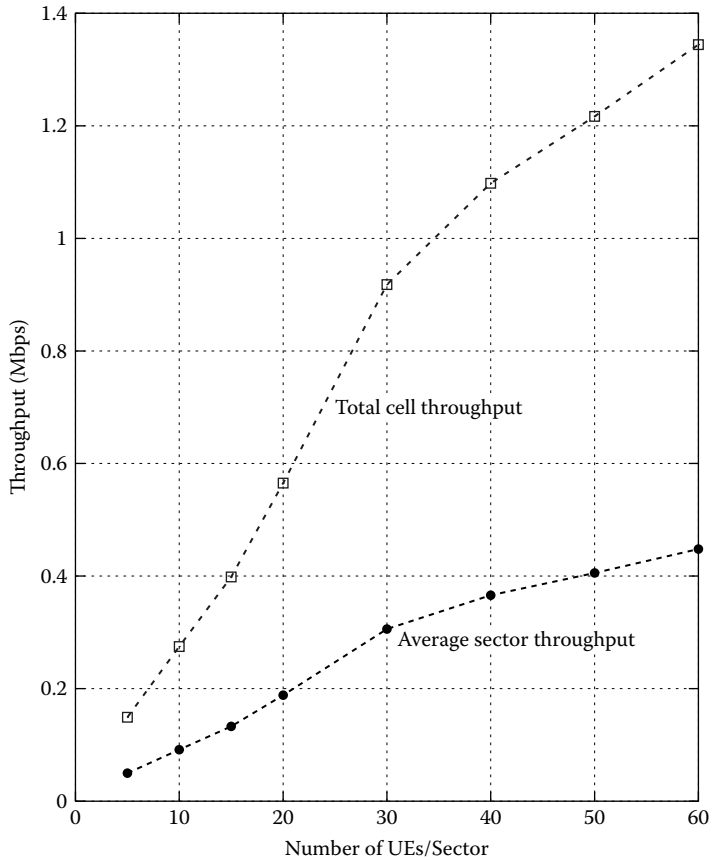

Figure 10.15 System throughput for the HSUPA, VoIP traffic.

The HSUPA system is very sensitive to co-channel interference. Therefore, the uplink scheduler should control the noise rise in the home-cell using the absolute or relative grant message. The HSUPA system provides high throughput through fast uplink scheduling at Node B, compared to the conventional WCDMA uplink.

References

[1] 3GPP. *Multiplexing and Channel Coding (FDD)*, 3GPP TS 25.212, v. 6.7.0. December 2005.

[2] International Telecommunication Union. *Guidelines for evaluation of radio transmission technologies for IMT-2000*, ITU Std. Rec.ITU-R M.1225, 1997.

[3] 3GPP. *Physical Layer Procedures (FDD)*, 3GPP TS 25.214, v. 6.3.0. September 2004.

[4] 3GPP. *UE Radio Access Capabilities*, 3GPP TS 25.306, v. 6.7.0. December 2005.
[5] 3GPP. *Physical Channel Mapping of Transport Channels onto Physical Channels (FDD)*, 3GPP TS25.211, v. 6.7.0. December 2005.
[6] *1xEV-DV Evaluation Methodology—Addendum (V6)*, WG5 Evaluation Ad-hoc Group Std. July 2001.
[7] IEEE 802.16 Broadband Wireless Access Working Group. *IEEE 802.16m Evaluation Methodology Document (EMD).* July 2008.